The LINNEAN SOCIETY of London BIOLOGICAL Journal of the Linnean Society

Biological Journal of the Linnean Society, 2013, ••, ••–••. With 7 figures

Disentangling the effects of intraspecies variability, phylogeny, space, and climate on the evolution of shell morphology in endemic Greek land snails of the genus *Codringtonia*

PANAYIOTA KOTSAKIOZI[1]*, FRANÇOIS RIGAL[2], EFSTRATIOS D. VALAKOS[1] and ARISTEIDIS PARMAKELIS[3]

[1]*Department of Animal and Human Physiology, Faculty of Biology, University of Athens, Panepistimioupoli Zografou, GR-15784 Athens, Greece*
[2]*Azorean Biodiversity Group, (CITA-A), Universidade dos Açores, Departamento de Ciências Agrárias, Rua Capitão João d'Ávila, São Pedro, 9700-042 Angra do Heroísmo, Terceira, Portugal*
[3]*Department of Ecology and Taxonomy, Faculty of Biology, University of Athens, Panepistimioupoli Zografou, GR-15784 Athens, Greece*

Received 11 June 2013; revised 7 July 2013; accepted for publication 7 July 2013

Extensive variation in land snail shell morphology has been widely documented, although few studies have attempted to investigate the ecological and evolutionary drivers of this variation. Within a comparative phylogenetic framework, we investigated the temporal and spatial evolution of the shell morphology of the Greek endemic land snail genus *Codringtonia*. The contribution of both inter- and intraspecies shell differentiation in the overall shell variability is assessed. The effect of climate, space, and evolutionary history on the shell variability was inferred using a variance partitioning framework. For *Codringtonia* species, intraspecies divergence of shell traits contributes substantially to the overall shell variability. By decomposing this variability, it was shown that the overall shell size of *Codringtonia* clades is phylogenetically constrained, related to early speciation events, and strongly affected by large-scale spatial variability (latitudinal gradient). The effect of climate on shell size cannot be disentangled from phylogeny and space. Shell and, to a larger extent, aperture shape are not phylogenetically constrained, and appear to be mostly related to conspecific populations divergence events. Shell shape is substantially explained by both climate and space that greatly overlap. Aperture shape is mainly interpreted by medium to small-scale spatial variables. *Biological Journal of the Linnean Society*, 2013, ••, ••–••.

ADDITIONAL KEYWORDS: latitudinal gradient – Peloponnese peninsula – phylogenetic signal.

INTRODUCTION

Land snails represent a challenging group for studying the evolution of shell morphological plasticity. They are known to exhibit great variability in shell shape, size, sculpture, and colour both at the inter and intraspecies level (Goodfriend, 1986; Suvorov, 2002; Stankowski, 2011). During recent decades, several studies have attempted to identify the ecological drivers and consequences of this shell variability. For example, shell size has been considered as one of the parameters that highly correlates with the distributional range size of many land snail species. It has been claimed that land snail species with larger shells tend to occupy wider distributional areas as a result of their greater dispersal capabilities, as well as their greater attractiveness as a prey, which, in turn, increases their passive dispersion (Pfenninger, 2004). However, the opposite has also been proposed, and there is much evidence to support it (Cameron *et al.*, 2011; Cameron, 2013). Additionally, shell variability

*Corresponding author. E-mail: pkotsakiozi@biol.uoa.gr

has been correlated with habitat (Chiba, 1996), competition and resource heterogeneity (Parent & Crespi, 2009), and climatic conditions, such as temperature and moisture (Goodfriend, 1986).

Although many studies have explored the relationship between shell variability and spatial and environmental factors (Alonso *et al*., 1985; Cameron, Cook & Gao, 1996; Chiba, 1996), only a few studies have attempted to quantify the contribution of the evolutionary processes in shaping the observed shell pattern (Hausdorf, 2003; Teshima *et al*., 2003; Jordaens *et al*., 2009; Kappes *et al*., 2009; Johnson, 2011; Okajima & Chiba, 2011). The correlation of shell variability with climate (Goodfriend, 1986) and habitat (Chiba, 1996) has been recorded in some species; however, it has also been claimed (Burla, 1984) that heritance contributes significantly as well. Moreover, it has been argued that the latitudinal pattern that land snail body size exhibits is not the result of repeated and independent evolution between body size and latitude but, instead, is a result of the predominance of some small size snails in one region and the presence of some other large body size individuals in another region (Hausdorf, 2003). As supported by Garland, Bennett & Rezende (2005), empirically, it makes sense that closely-related species tend to be more similar than distantly-related species. Therefore, by applying this rational to land snails, it is anticipated that closely-related species are more likely to share common shell characters (size, traits, etc.) than distantly-related species. On the other hand, there are cases where rapid evolution of diversity in biological traits has led closely-related species to be morphologically distinct. Two types of rapid evolution (radiation) can be distinguished: the adaptive in which the usage of different sources and different ecological parameters can lead to different (morphological and/or physiological) characteristics and the non-adaptive radiation that leads to differentiation without any respective ecological specialization (Schluter, 2006). Consequently, whenever a comparative analysis is conducted, the phylogenetic relationships of the species involved should be taken into account. This could help to decipher whether the observed variability is, to some extent, disconnected from the genetic heritance (i.e. which could refer to adaptation or if it can be fully explained by the phylogenetic hierarchy of the studied taxa) (Garland *et al*., 2005). Nevertheless, in such an approach, major issues can arise; for example, how to properly account for the intraspecies variation, which is a frequently neglected aspect (Ives, Midford & Garland, 2007). Indeed, assuming that the phenotypic mean of a trait is species-specific indirectly implies that the intraspecies variation is absent or negligible (Ives *et al*., 2007; Garamszegi & Møller, 2010). However, this is not always the case and, especially for groups such as land snails that exhibit extensive shell variability at the intra- and interspecific level, within-species variation should not be neglected. Moreover, as has been shown for the interspecific level, intraspecies variability can also be controlled by ecological factors that might be essential for identifying all the forces that shape a trait's variability. Consequently, considering that the intraspecies variability of a trait is not negligible, any trait variation must be investigated in regard to its intra- and interspecific component, and the contribution of each component should be evaluated separately (Stevens, Pavoine & Baguette, 2010).

In the present study, within a comparative phylogenetic framework, we investigated the temporal and spatial evolution of the shell morphology of the recently radiated (Kotsakiozi *et al*., 2012) land snail genus *Codringtonia* Kobelt 1898 in continental Greece. *Codringtonia* is endemic to Greece and has a restricted and mosaic distribution in the Peloponnese peninsula and Central Greece (or Sterea Ellada) (Subai, 2005). The latter study defined eight *Codringtonia* species, one of them assigned to a different subgenus, using morphological characters of the shell and the genitalia system. However, the recently resolved mitochondrial DNA phylogeny revealed that the eight nominal species correspond to six phylogenetic clades because two nominal species are forming one monophyletic clade, whereas the species assigned by Subai (2005) to a different subgenus probably belongs to a different genus distantly related to *Codringtonia* (Kotsakiozi *et al*., 2012). At this point, it is interesting to note that, in a relatively small geographical region occupied by this endemic genus and in a short period of time, six clades (attributed to seven nominal species) were formed (Kotsakiozi *et al*., 2012). Therefore, the issue emerging and meriting further investigation is what was the tempo and mode of shell differentiation that was coupled with the radiation of the genus? To assess this question and disentangle the effects of phylogeny, stochasticity and adaptation in the variability of the shell, we aimed to investigate: (1) do different *Codringtonia* species occupy a distinct position within the morphological space of the genus; (2) how does intraspecies shell variation affect the shell variability of *Codringtonia* clades; (3) is intra- and interspecific shell variability related to any spatial or (contemporary and past) climatic factors; (4) to what degree does phylogenetic affinity affect the shell differentiation between and within *Codringtonia* clades; and (5) how is shell variation partitioned along the phylogenetic history of *Codringtonia*'s radiation?

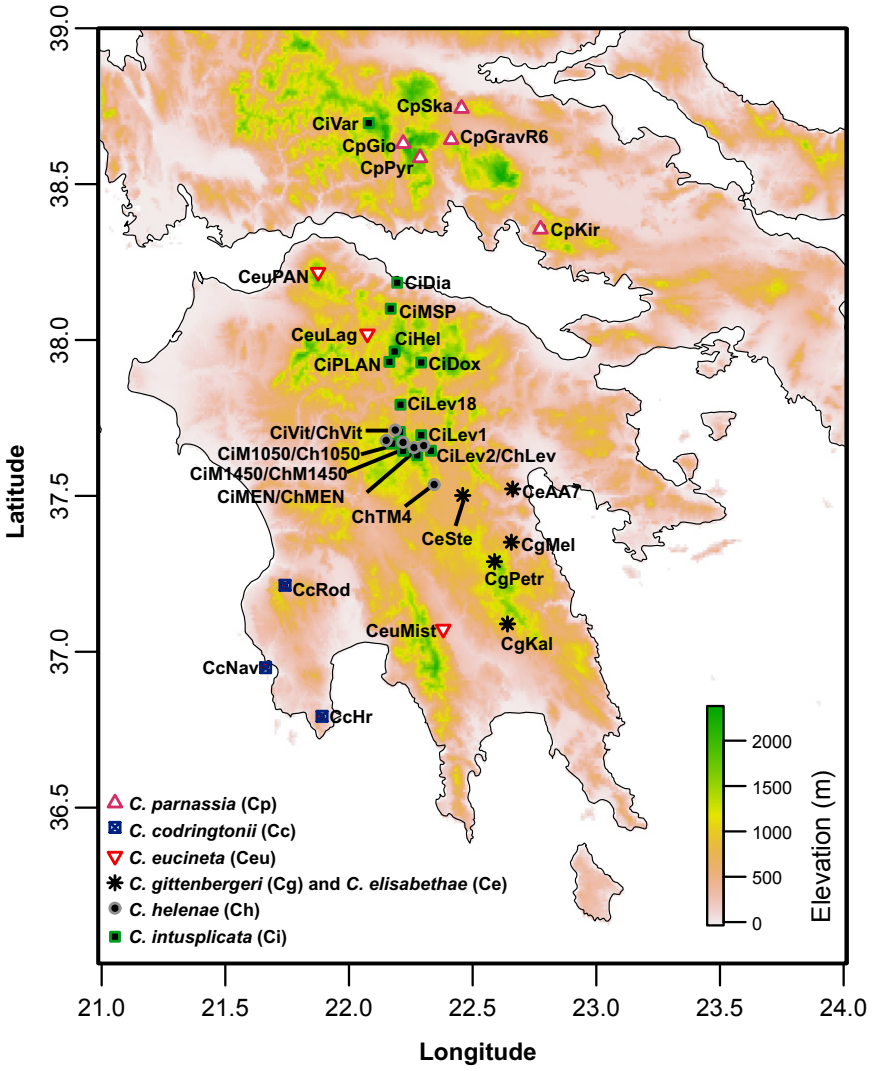

Figure 1. Geographical localities of the *Codringtonia* species populations included in the present study. The map codes correspond to those provided in the Supporting information (Table S1). The different populations of each single species are indicated by different symbols, as shown in the legend. The location for population CiVar is indicative because no geospatial information was available for these museum specimens.

MATERIAL AND METHODS

CODRINGTONIA SAMPLES, SHELL MEASUREMENTS, SPATIAL AND CLIMATIC DATA OF SAMPLED LOCALITIES

The analyses performed in the present study rely on the *Codringtonia* species delimitations reported in the phylogenetic analysis of Kotsakiozi *et al.* (2012). Briefly, the genus *Codringtonia* is comprised of six phylogenetic clades that correspond to seven nominal *Codringtonia* species. In essence, two nominal species, namely *Codringtonia gittenbergeri* and *Codringtonia elisabethae*, cluster together forming one monophyletic clade, whereas the remaining species (*Codringtonia codringtonii*, *Codringtonia eucineta*, *Codringtonia helenae*, *Codringtonia intusplicata*, and *Codringtonia parnassia*) each correspond to a different clade. The temporal evolution of the shell features of *Codringtonia* is focused on species and population level. Ultimately, we were able to obtain shells from 35 populations (Fig. 1; see also Supporting information, Table S1) with a minimum of three shells (in two out of the 35 populations) per population and a total of 394 adult individuals of all *Codringtonia* species. We should note that each nominal species corresponds to a different clade according to the phylogeny of the genus but, because *C. gittenbergeri* and *C. elisabethae* form one monophyletic clade, we refer to them as *C. gittenbergeri-elisabethae*. When the collecting

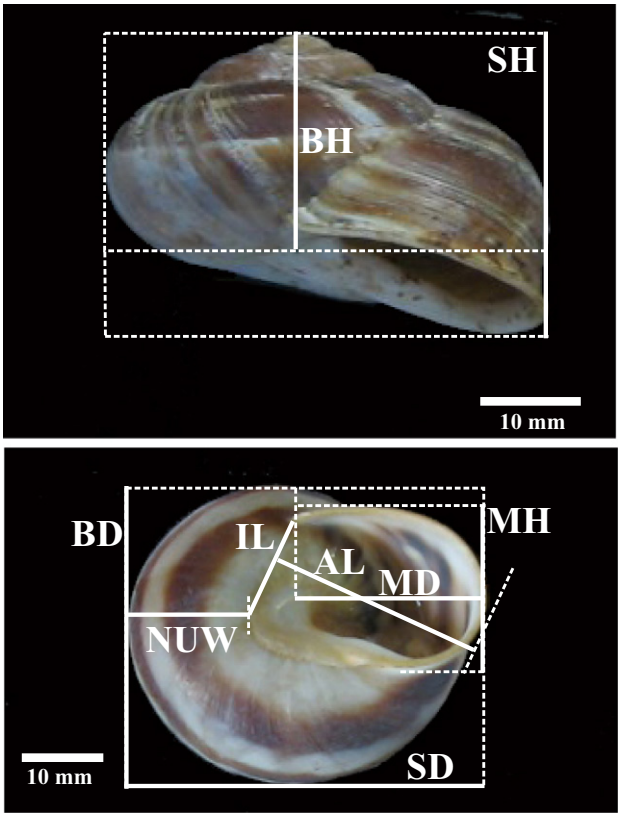

Figure 2. The variables measured on the shells of *Codringtonia* specimens. The dashed lines indicate the start and end points of the measured variables (continuous lines). BH, body height; SH, shell height; BD, body diameter; SD, shell diameter; MH, aperture height; MD, aperture diameter; NUW, non-umbilicus width; IL, inner lip length; AL, aperture length.

efforts from the field were not successful, we complemented our specimens using material loaned from European museums. Our field collecting trips were performed in accordance with the description of the sampling localities of Subai (2005). The latter study examined specimens of *Codringtonia* mostly maintained in European museums and private collections. Therefore, requesting museum samples that would complement our own collections was a straightforward process. With the exception of two sampling localities, latitude, longitude, and altitude were recorded for each locality (see Supporting information, Table S1). Specimens were assigned to species based on a combination of characters, including shell measurements, sculpture and colour, genitalia features, and location of origin. Images of each individual specimen were taken using a digital camera, always including a length scale. Nine shell measurements were taken from each specimen (Fig. 2). Measurements were taken using IMAGEJ (http://rsbweb.nih.gov/ij/index.html) and were chosen to express (1) body size and shape, and these were shell and body height (SH and BH, respectively), shell diameter (SD), body diameter (BD), and non-umbilicus width (NUW); (2) aperture size and shape, as defined by aperture (or mouth) diameter (MD), aperture height (MH), aperture length (AL), and length of inner lip (IL); and (3) two ratios, SH/SD and MD/MH (Fig. 2). The ratio SH/SD is also known as the spire index (SI). As Chiba & Kaustuv (2011) report, field observations and laboratory experiments have indicated that the spire index plays a functional role leading to microhabitat preferences, with high-spired species tending to be active on steep or vertical surfaces, and low-spired species preferring low-angle or horizontal substrates. In addition, a theoretical model of shell shape has suggested that low-spired species are optimized for locomotion on horizontal surfaces, whereas both low- and high-spired species can be well balanced on vertical surfaces. For all analyses involving a phylogenetic framework and for which branch lengths were required, we restricted the analyses to the populations (see Supporting information, Table S1) present in the dated phylogeny provided by Kotsakiozi *et al*. (2012) (see Supporting information, Fig. S1). This reduced our dataset to 19 populations with three populations per species, except for the species of *C. intusplicata* for which four populations were considered.

Climatic variables for the sampled localities were extracted from WorldClim interpolated climate surface (http://www.worldclim.org/; Hijmans *et al*., 2005). We considered the present conditions (resolution 30 arc-s) and data for the last glacial maximum (LGM; approximately 21 000 years ago; resolution 2.5 arc-min). For LGM predictions, we used data from both the Community Climate System Model (CCSM) and the Model for Interdisciplinary Research on Climate (MIROC). The WorldClim database provides 19 bioclimatic variables (see Supporting information, Table S2). For each dataset (i.e. contemporary climate and two datasets for the LGM), a principal components analysis (PCA) was performed on the Pearson's correlation matrix of the data to reduce the dimensionality of the highly correlated climatic data. The first three components produced by the PCA (called hereafter CC1, CC2, and CC3 for the Contemporary Climate; LGM_M1, LGM_M2, and LGM_M3 for MIROC; and LGM_C1, LGM_C2, and LGM_C3 for the CCSM model) accounted for more 97% of the variance of the 19 climatic variables in all cases (see Supporting information, Table S3) and were kept as composite climatic variables in our subsequent analyses. We should note that the palaeoclimatic conditions during the last interglacial period (120 000 years ago) were in many respects similar to the contemporary ones of the Mediterranean basin as has been reported for the

Western Mediterranean as well (Bardají *et al*., 2009), and were not considered in the present study.

Morphological differentiation between species

The morphological differentiation of *Codringtonia* species was assessed using all the obtained individual shell measurements (N = 394). A PCA on the Pearson's correlation matrix containing the nine log-transformed measurements and the two ratios was performed. Log-transformations were applied to meet the requirements for the statistical analysis with parametric methods and to minimize probable distortion caused by allometric relationships of the variables. The ratios were kept untransformed because no deviation from normality was observed. Because the nine shell measurements and the two ratios were substantially correlated, we selected the first three PCA scores (hereafter SH1, SH2, and SH3) as composite expressions of the shells' morphology and they were used in all subsequent analyses. Based on the PCA scores and to verify the visually observed separation of *Codringtonia* species in the PCA diagram, we performed a nonparametric permutational multivariate analysis of variance (PerMANOVA; Anderson, 2006) using the scores of the individuals for the first three principal component of the PCA as dependant variables and species-clades as the explanatory factor. PerMANOVAs were then run for all the SH axes together and each SH axes separately. PerMANOVA is a statistical framework that does not rely on strict assumptions that are difficult to be met when analysing samples of different size. PerMANOVA partitions the sums of squares of multivariate data sets in a manner similar to the standard analysis of variance, except that it can use any distance metric between samples to compute the sums of squares (Anderson, 2006). If the observed pseudo-F-value is higher than 5% of the null distribution of the pseudo-F-values then H_O is rejected. Here, we used Euclidean distances and estimated the p-values using 10 000 iterations. If the overall test is significant, post-hoc pairwise PerMANOVA tests can be performed to identify significant differences among species. In the post-hoc significance tests implemented in the PerMANOVA analysis, we applied the sequential Holm (Holm, 1979) correction to avoid false positive results that could occur in pairwise tests.

Intra- and interspecies shell variability

For the estimation of the contribution of both species and populations on the total shell morphological variability, an ANOVA-like statistic test with nested design could not be applied (Ricklefs, 2012) because our dataset is unbalanced at population level (i.e. not the same number of populations per species and strong variation in the number of individuals used per population). Therefore, we used the test proposed by Stevens *et al*. (2010) and we partitioned the shell variability across the phylogenetic tree by measuring the relative contribution of intra- and interspecific nodes to the total shell variability. The contribution of a given internal node to the trait diversity is equal to the diversity in trait values among the clades that descend from that node multiplied by the proportion of species that descend from that node. Total shell variability and the contribution of the intra- and interspecies nodes were calculated by using Rao's quadratic entropy (Rao, 1982; Stevens *et al*., 2010). This analysis was conducted using the mean values of the shell variables for each population. We first applied the visual methodology proposed by Pavoine, Baguette & Bonsall (2010) in which the plotted contribution of each node in the tree gives a graphical representation of the diversity at different depths in the phylogenetic tree. Second, to specifically test the contribution of populations to the total shell morphological variability, we summed all the variability associated to the intraspecific nodes for all species (i.e. the observed intraspecific variance) and then we permuted values of the trait across the tips of the phylogeny, meaning that the trait values are randomly exchanged among all species. The null hypothesis of this test is that the diversity in trait values among the species that descend from an interspecific node is equivalent to the diversity in trait values among the populations that descend from an intraspecific node. We repeated this permutation process 1000 times. For each permutation, we re-computed the intraspecific variance and then compared the observed intraspecific variance with the simulated values. The intraspecific variation was considered lower than expected by chance if less than 5% of the simulated values were lower or equal to the observed value. All statistics were performed for both the three first SH axes together and independently to test whether all the dimensions of the morphological variability are distributed equally across the phylogeny. Because this method does not consider branch lengths but only tree topology (Stevens *et al*., 2010), and because each species represents a monophyletic clade, we used the 35 populations by constructing an enlarged phylogenetic tree in which each population was artificially grafted to its corresponding species.

Phylogenetic signal and patterns of traits diversification

All of the subsequent analysis take into account branch lengths; therefore, we only considered the 19

populations for which phylogenetic information was available (Kotsakiozi *et al*., 2012). To quantify the amount of phylogenetic signal for each shell variable, SH1, SH2, and SH3, we calculated the metric K of Blomberg *sensu* Blomberg, Garland & Ives (2003). This metric compares the observed and expected levels of phylogenetic signal in a continuous vector, assuming that the traits evolve following a Brownian motion. If K is > 1, then close relatives are more similar in trait values than expected from a Brownian mode of evolution, whereas, if K is < 1, close relatives are less similar than expected. We also applied the randomization procedure proposed by Blomberg *et al*. (2003) to test whether the shell variability exhibits a significant tendency to be similar in related species/populations. To account for intrapopulation variance, which can sometimes greatly influence our perception of phylogenetic dependency (Hardy & Pavoine, 2012), we estimated K by integrating the SE *sensu* Ives *et al*. (2007). To complement our analysis of phylogenetic signal, we also implemented the phylogenetic signal-representation approach (PSR) proposed by Diniz Filho *et al*. (2012). This new method derived from the phylogenetic eigenvector regression analysis (PVR; Diniz-Filho, De Sant' Ana & Bini, 1998) in which eigenvectors are extracted from a phylogenetic distance matrix and used to model interspecific variation. Because the phylogenetic eigenvectors are orthogonal, each one depicts a particular pattern of relationships among the lineages considered. For example, the first eigenvectors associated with the largest eigenvalues represent the largest phylogenetic distances (usually the distances between the main clades closer to the root) and, progressively, eigenvectors with smaller eigenvalues are associated with smaller phylogenetic distances. In the PSR method, the phylogenetic eigenvectors are successively added in a series of linear models and then the R^2 of those sequential models are plotted against the cumulative some of the eigenvalues. By using simulations and empirical data, Diniz Filho *et al*. (2012) have shown that a linear relationship is expected under Brownian motion, whereas a PSR above the linear expectation corresponds to a process of early diversification (acceleration is such that the early clades tend to diverge more than expected early in the phylogeny), and a PSR below indicates a pattern of recent diversification (clades tend to diverge from each other late in the tree). As a measure of the deviation from the Brownian expectation, Diniz Filho *et al*. (2012) suggested to use the area under the curve (AUC) between the 45° line and the cumulative R^2 with a negative AUC being associated with traits evolving slower (and a positive AUC being associated to traits evolving faster) than expected under Brownian motion. Diniz Filho *et al*. (2012) also showed that the AUC values in PSR plots are strongly correlated with the K of Blomberg, although one of the advantages of this method is that it also provides elegant graphics for a better visualization of the deviations from the Brownian motion in terms of accelerations or decelerations of the evolutionary rate occurring along the phylogeny. Thus, the patterns of traits diversification are easier identified. *Sensu* Diniz Filho *et al*. (2012), the AUC values were also used to specifically test: (1) whether the trait evolution deviated significantly from the Brownian motion model by comparing the observed AUC to 1000 AUCs generated by simulating continuous traits along the phylogeny under a Brownian motion model and (2) whether the trait evolution deviated significantly from the null expectation i.e. absence of phylogenetic signal by comparing the observed AUC to 1000 AUC generated by randomizing traits values across species. To perform this analysis, we extracted the phylogenetic eigenvectors by applying a PCA on the double-centred phylogenetic distance matrix containing the pairwise distances between populations derived from the dated phylogeny with the 19 populations.

Modelling shell morphological variability: the relative contribution of climate, space, and phylogeny

We first explored the association between shell variability and latitude/longitude in a phylogenetic framework. Even though latitude and longitude are considered in the variance partitioning analysis (see below), they are transformed in such a way that it is not easy to interpret their relationship with shell variability. On the other hand, testing the association of these variables with the untransformed longitude/latitude data allowed us to investigate whether a broad spatial trend is evident in SH1, SH2, and SH3. To achieve this, we performed phylogenetic generalized least squares (PGLS) regressions (Garland & Ives, 2000) to account for potential phylogenetic dependence between the shell (SH1, SH2, SH3) and the spatial variables. PGLS assumes that residual variation among species is phylogenetically correlated and estimates the parameter (lambda) λ (i.e. automatically estimated with other parameters of the model by maximum likelihood), which indicates the degree of phylogenetic dependence in the data. Values of λ vary between zero and one. A value of zero is pointing to a differentiation pattern that is independent of the phylogeny (i.e. results equal to those provided by the ordinary least square method), whereas a value of one indicates a Brownian model of change. In the subsequent analysis, we quantified the relative contribution of the climatic conditions, space and phylogeny in determining shell morphological

variability by using a variance-partitioning framework (Legendre & Legendre, 1998). Variance partitioning led to splitting the variance of the response variable (here, SH1, SH2, and SH3) into components explained solely by the effects of two or three explanatory datasets (here, climatic conditions, spatial variables, and phylogeny), representing components explained by their combined effects and finally the unexplained component (i.e. residuals). This analysis considers two steps: (1) modelling shell morphological variability as a function of climate conditions, space and phylogeny separately. Each of these models contains a set of explanatory variables that are specifically selected independently of the other two sets of variables and (2) combining the three models in variance partitioning analysis. Here, the partitioning of the variance was based on linear regression and using the adjusted R^2 because it provides unbiased estimates. The effect of climate conditions was modelled by using the composite variables for both contemporary climatic conditions and for the LGM climatic conditions. Because two sets of variables derived from two distinct climatic models were available for the LGM, we re-run the subsequent analysis by including separately each of them. We undertook preliminary data exploration to identify possible high collinearity between contemporary and LGM climatic variables. We computed the variance inflation factor (VIF) and we sequentially dropped the variable with the highest VIF, recalculated the VIFs and repeated this process until all VIFs were smaller than a preselected threshold. Here, we chose a threshold of 10, a less stringent value generally indicator of a 'severe' collinearity (Neter, Wasserman & Kutner, 1990). The procedure led to the exclusion of $LGM_{C/M}1$, which was found to be highly correlated with CC1 ($r = 0.94$ and $r = 0.93$ for LGM_M1 and LGM_C1, respectively). This means that, for this dimension, current and past climatic conditions were indistinguishable. For all other dimensions, VIF was found either equal or lower than 5.1, suggesting substantial independence between current and past conditions. To model the effect of space, we obtained spatial variables from principal coordinates of Neighbour matrices (PCNMs) (Borcard *et al*., 2004). The PCNM method is based on a spectral decomposition of the study area into a series of eigenvectors each representing a spatial scale. PCNM derived those eigenvectors from a PCA applied on the truncated matrix of geographical distances calculated with the latitude and longitude of the studied sites (Borcard & Legendre, 2002). As is true for PVR, PCNM vectors associated with larger eigenvalues represent broadscale patterns (e.g. north–south gradient in the study area), whereas PCNM vectors associated with smaller eigenvalues represent finer spatial scales. To model the phylogenetic effect, we used the phylogenetic eigenvectors produced for the implementation of the PSR (see above). For PCNM and PVR, multicollinearity was not investigated because all these axes are by definition orthogonal to each other. Subsequently, an information-theoretic approach was employed to capture the most important climatic, spatial and phylogenetic predictor(s) explaining each shell variable (SH1, SH2, and SH3). All possible models (i.e. $N = 2^x$ for X variables corresponding to all possible combinations of predictors, including the null model) were fitted and Akaike's information criterion corrected for small sample size (AICc) (Sugiura, 1978) was calculated for each model. AICc values were used to estimate the Akaike weights (w_i) for each model. We used Moran's I tests and the inverse cophenetic distance matrices to ensure that the residuals of the phylogenetic model after forward selection did not show signs of phylogenetic autocorrelation and, similarly, that the residuals of the spatial model did not show signs of spatial inertia using the inverse of the geographical distance matrix (Cliff & Ord, 1981). On the best model selected, we applied simple or multiple linear regressions to test the effect of each of the retained variables. Variance partitioning was then implemented by combining the three reduced sets (i.e. one for space, one for phylogeny, and one for climate).

Statistical analysis

All of the statistical analyses performed in the present study were implemented within the R programming environment (R Development Core Team, 2011). Tree manipulations were achieved using the APE package (Paradis, Claude & Strimmer, 2004). The trait decomposition along the phylogenetic tree was performed by using the R code provided by Pavoine *et al*. (2010). K of Blomberg was computed using the PHYTOOLS package (Revell, 2012). Model selection was performed by using the MUMIN package (Barton, 2013). The PerMANOVA, PCNM and variance partitioning were performed using VEGAN (Oksanen *et al*., 2007). PVR and PSR analysis were performed using PVR (Santos *et al*., 2012).

RESULTS

Morphological differentiation between species

The plot of the PCA for all individuals included in the analysis is presented in Figure 3. The three PCA axes, PC1, PC2, and PC3 (referred to as SH1, SH2, and SH3, accordingly) explained 62.64%, 15.15%, and 10.4% (a total of 88.2%) of the total shell variability, respectively, whereas each of the remaining axes explained less than 4% of the variance. According to the contribution of each of the raw variables (Table 1),

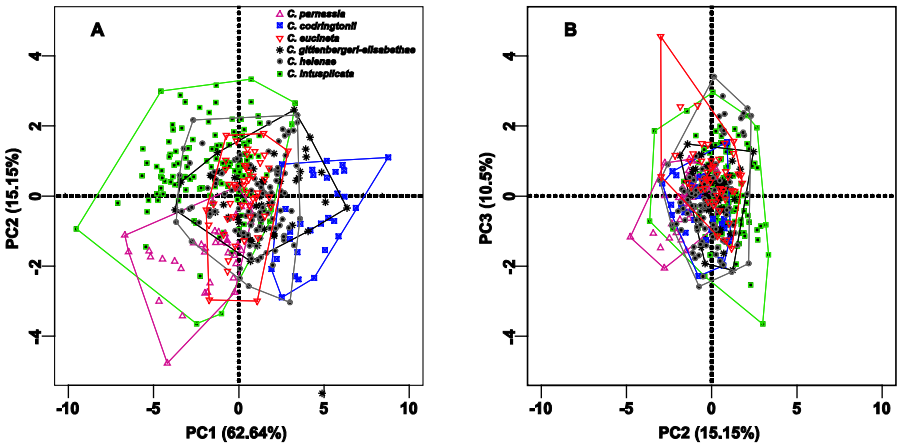

Figure 3. Scatter-plot of the scores of the principal component analysis (PCA) on the first three principal components (PCs) accounting for 88.2% of the total shell variation of the six *Codringtonia* species studied. The polygons define the morphological space occupied by each species. A, scatter-plot with PC1 and PC2. B, scatter-plot with PC2 and PC3.

Table 1. The contribution (loadings) of each shell variable on the first three principal component axes SH1, SH2, and SH3

	SH1 (62.64%)	SH2 (15.15%)	SH3 (10.4%)
SD	**0.958**	0.173	0.022
SH	**0.897**	–0.302	–0.282
BD	**0.924**	0.341	0.017
BH	**0.899**	–0.296	–0.209
MD	**0.823**	0.418	–0.162
MH	**0.852**	–0.108	0.477
AL	**0.829**	0.183	0.066
IL	**0.759**	–0.200	–0.055
NUW	**0.740**	0.423	0.015
SH/SD	0.399	**–0.788**	–0.427
MD/MH	–0.364	**0.531**	**–0.759**

The percentage of variance explained by each principal component is given in parentheses. Contribution values above 0.5 are indicated in bold.

SH1 is an expression of the shell's overall size. The loadings of the shell variables on SH1 are greater than 0.8 with the exception of NUW, IL, and the ratios SH/SD and MD/MH (Table 1) that have loadings below this value. Consequently, individuals with smaller shell sizes are on the left side of the SH1, whereas those of greater shell size are on the right side of SH1. SH2 is dominated by the contribution of the ratio SH/SD (also known as spire index, SI) that exhibits a loading value of 0.788 (Table 1). Therefore, SH2 can be considered an expression of the shell's shape. Individuals that have a compressed shell (small values of SH/SD) are on the upper part of SH2, whereas those with a less compressed (elongated) shell are on the lower part of SH2 in Figure 3A. SH3 is dominated by the ratio MD/MH with a correlation of –0.759; therefore, SH3 can be considered as an expression of the shape of the shell's aperture. Individuals that have an ellipsoid aperture (MD/MH above 1) are on the lower part of Figure 3B, whereas individuals with a more roundish aperture (MD/MH close to 1) are on the upper part of Figure 3B. Both the results of the PerMANOVA based on the three axes and for each axes separately indicated that species differed significantly in their shell morphology (All: $R^2 = 0.38$, $F_{5,388} = 47.15$, $P < 0.001$; SH1: $R^2 = 0.46$, $F_{5,388} = 65.39$, $P < 0.001$; SH2: $R^2 = 0.27$, $F_{5,388} = 28.79$, $P < 0.001$; SH3: $R^2 = 0.06$, $F_{5,388} = 4.64$, $P < 0.001$). The results of the post-hoc tests using PerMANOVA for species pairwise comparisons are provided in the Supporting information (Table S4). These tests are also in favour of significant differences being present between species pairs.

Decomposition of the shell morphology along the phylogeny: the relative contribution of species and populations

The results of the decomposition of the shell's morphological variability into species and populations are given in Figure 4 and in Table 2. We found that populations account for more than 50% of the variance for both all variables together and independently. However, our permutations tests revealed that only for aperture shape (SH3) was the observed variance not significantly different from a random distribution of traits among the nodes of the tree, indicating that variation attributable to the population level was not different from that observed at the interspecific level. On the other hand, for shell size (SH1) and shell

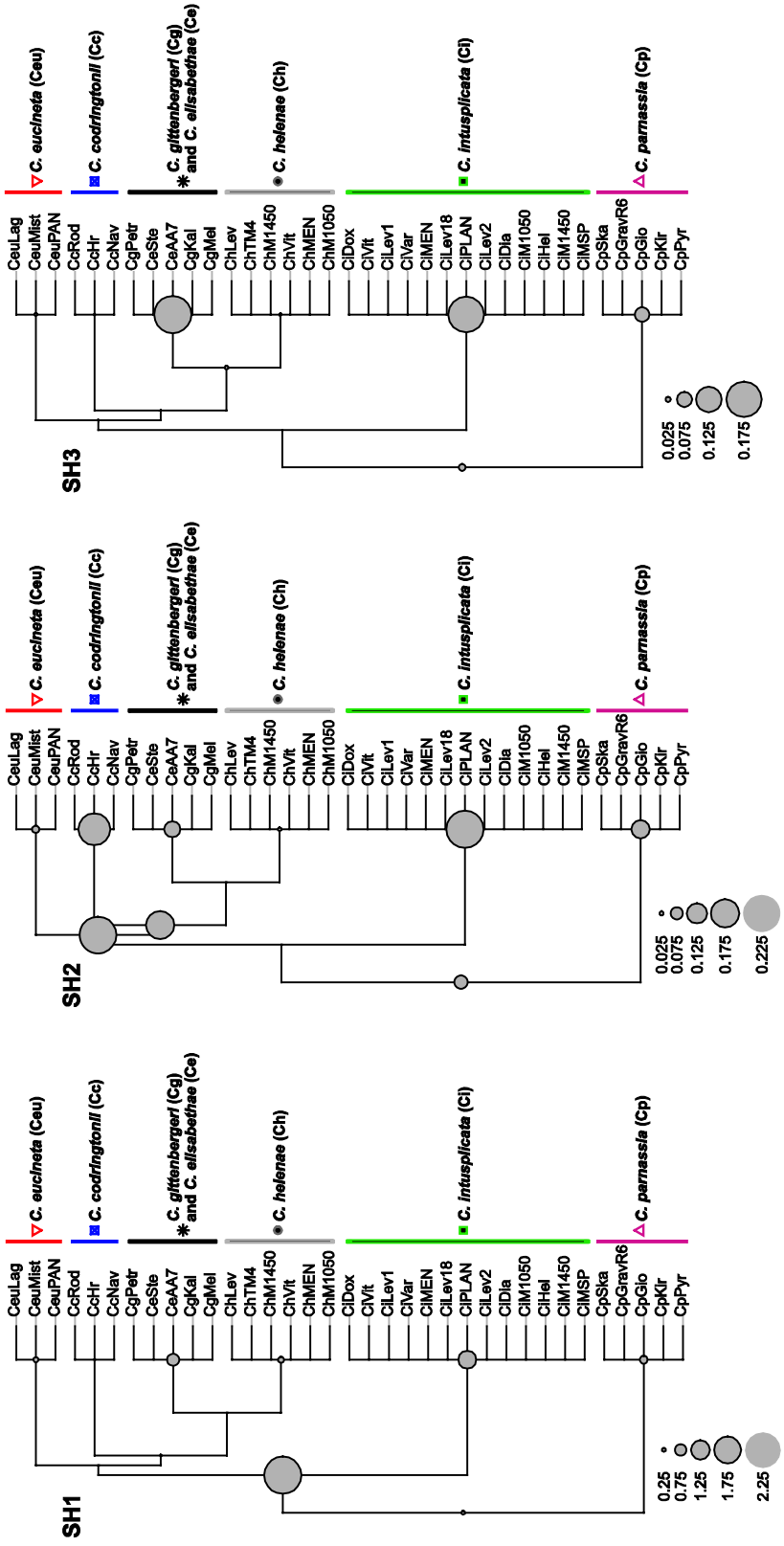

Figure 4. Decomposition of the shell variability along the *Codringtonia* phylogeny. The area of the circles at the nodes is proportional to the contribution of the nodes to the total shell variability (expressed by Rao's quadratic entropy). The scale is given at the bottom of the panels.

Table 2. Partitioning of the shell morphological diversity between species and populations along the phylogeny of *Codringtonia*

Variables	Amount of variance		%	Lower bound	*P*
	Total	Population			
ALL	7.78	4.72	61	5.68	0.003
SH1	6.06	3.54	58	4.28	0.002
SH2	1.19	0.68	58	0.82	0.008
SH3	0.52	0.49	95	0.36	0.921

Partitioning was assessed for the three (SH1, SH2, and SH3) composite shell variables together (ALL) and for each one of them independently. We considered an artificial tree in which all of the populations available ($N = 35$) were grafted to their respective species, assuming a full polytomy within each species. The partitioning was computed by using the Rao quadratic entropy. The total variance, as well as the amount of variance (and percentage of total variance) explained by the populations is given. Permutation tests were performed with 1000 permutations. The 5% lower bounds and the associated *P*-values are given.

shape (SH2) and when all variables were considered together, the variance attributed to the population level was lower than expected by chance, meaning that the variance attributable to populations was significantly lower than the one attributable to interspecific level.

Phylogenetic signal and patterns of traits diversification

The *K*-statistic was below one for all shell variables (SH1 = 0.475, SH2 = 0.351, and SH3 = 0.484), meaning that, for all cases, species/populations under study are less similar than expected. Moreover, only shell size (SH1) displayed a significant phylogenetic signal according to the randomization test ($P = 0.022$). Results of the PSR method are given in Figure 5. The PCA performed on the cophenetic distance matrix from the dated tree generated 18 eigenvectors and all of them were retained in the subsequent analyses. Each eigenvector depicts a particular pattern of relationships among the populations, with the first eigenvectors being associated with the largest phylogenetic distances and the last eigenvectors with smaller phylogenetic distances. For shell size, the relationship between the R^2 from the sequential models and the cumulative sum of the eigenvalues followed approximately the 45° line. This is reflected in the small positive value of AUC (0.03). Null simulations based on the AUC values showed that shell size was significantly related to the phylogeny (null model under the hypotheses of an absence of phylogenetic signal $P = 0.001$) but does not differ from a Brownian motion model of evolution ($P = 0.275$). For shell shape (SH2), the curve was below the Brownian expectation, with at least more than 50% of the variance explained by the last 14 eigenvectors representing less than 20% of the total inertia of the phylogeny. The deviation is reflected in the negative AUC (–0.09) but no deviation from the Brownian expectation was found ($P = 0.694$). As for shell size, shell shape was also found to be phylogenetically dependent (null model under the hypothesis of an absence of phylogenetic signal for AUC; $P = 0.009$). The pattern for aperture shape (SH3) is even more pronounced than that for shell shape, with most of the variance being explained by the last 15 eigenvectors representing less than 30% of the total inertia of the phylogeny. This pattern is clearly reflected in the AUC (–0.24). Aperture shape was found to be significantly independent of the phylogeny (null model under the hypotheses of an absence of phylogenetic signal for AUC; $P = 0.22$) but did not deviate from the Brownian motion model of evolution ($P = 0.961$).

Relative contribution of climate, space, and phylogeny in determining the variability of the shell

The results of the PGLS applied between each shell variable and latitude and longitude showed that only shell size (SH1) was negatively and significantly explained by latitude (PGLS: $R^2 = 0.39$, $F_{2,17} = 11.18$, $P < 0.001$). According to the loadings (Table 1) of shell size, larger individuals are located in the south of the distributional area, with smaller individuals found in the northern part (Fig. 6). The λ value of this relationship was equal to 0.187 with no significant deviation from 0 ($P = 0.80$) but significantly different from 1 ($P < 0.001$). Thus, this relationship does not appear to be affected by the phylogenetic affinities of the populations involved.

Results of the best model selected for the phylogenetic, spatial and climatic set of predictors are given in Table 3. Model coefficients for each selected variable are given in the Supporting information (Table S5). For the climatic model, CC1 and LGM_C2 were selected as the best predictors for shell size (adjusted $R^2 = 0.388$, $P = 0.007$). Only LGM_C3 was retained for shell shape (SH2) (adjusted $R^2 = 0.352$, $P = 0.004$), whereas no climatic predictor was kept for aperture shape (SH3) after the model selection procedure. Similar results were found with the climatic variables extracted from the MIROC models (data not shown). The PCNM analysis allowed 11 PCNM eigenvectors to be obtained. The plot of each PCNM on the study area is shown in the Supporting

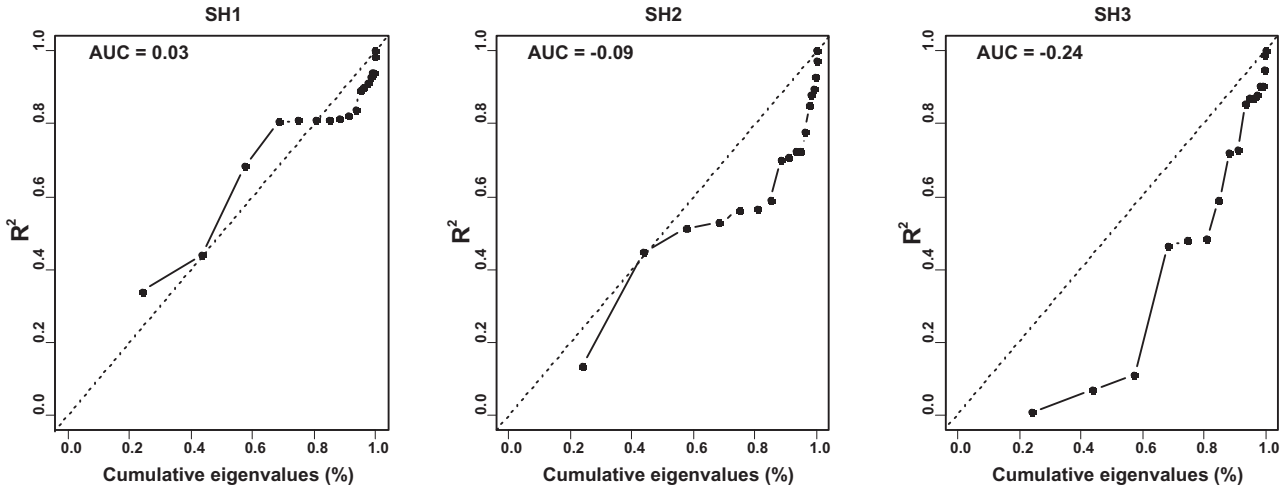

Figure 5. Phylogenetic signal-representation approach curves (solid line and circles) for SH1, SH2, and SH3 derived from the phylogenetic eigenvectors regressions incorporating successively eigenvectors. *Y*-axes represent the R^2 of the sequential models and *X*-axes represent the cumulative sum of the eigenvalues. The dotted line is the 45° line indicating the Brownian expectation. The values of the areas under the curves are given.

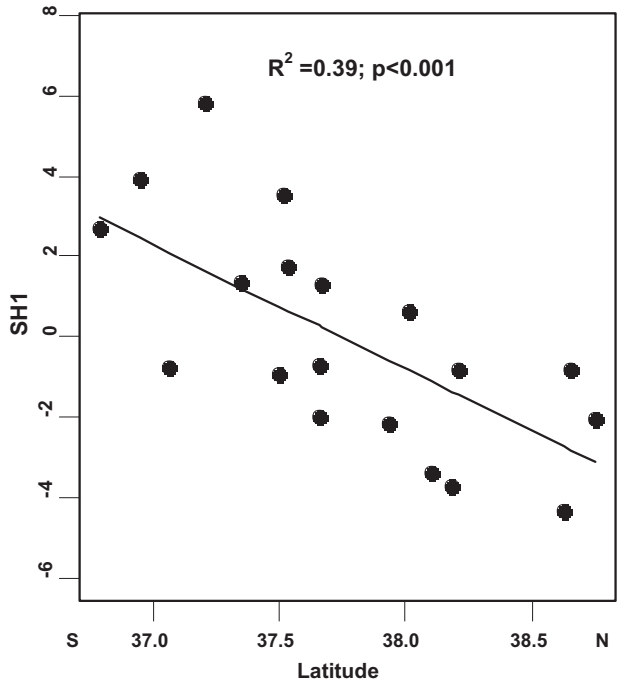

Figure 6. Relationship between latitude and SH1. The solid line corresponds to the predicted values from phylogenetic generalized least squares. The symbols 'N' and 'S' on the *X* axis indicate the North and South, respectively.

information (Fig. S2). Because PCNM eigenvectors may be interpreted as a decreasing gradient of broadscale spatial structures, we can arbitrarily group PCNMs from 1 to 3 as spatial broadscale vectors. For example, PCNM2 was significantly correlated with latitude ($r = 0.57$), whereas PCNM3 was significantly correlated with latitude and longitude ($r = 0.62$ and $r = 0.78$, respectively). PCNMs from 4 to 6 can be attributed to medium spatial scale, whereas PCNMs form 7 to 11 to small spatial scale. For the spatial model, PCNM 1, 2, 3, 7 and 8 were selected for shell size (adjusted $R^2 = 0.797$, $P < 0.001$). For shell shape, only the PCNM 1 was selected (adjusted $R^2 = 0.303$, $P = 0.008$), whereas PCNM 4 and 6 were retained for aperture shape (adjusted $R^2 = 0.521$, $P < 0.001$). For the phylogenetic model, the PVRs from 1 to 4 and PVRs 11 and 17 were selected for shell size (adjusted $R^2 = 0.856$, $P < 0.001$). For shell shape, PVRs 1, 2, and 8 were retained (adjusted $R^2 = 0.471$, $P = 0.005$), whereas PVRs 4, 7, 8 and 10 were maintained for aperture shape (adjusted $R^2 = 0.642$, $P < 0.001$). The variables selected to model phylogeny and space efficiently removed phylogenetic and spatial autocorrelation because Moran *I* tests were all nonsignificant for the three response variables SH1, SH2, and SH3 ($P > 0.2$). The results of the variance partitioning are shown in Figure 7 (see also Supporting information, Table S6). For shell size, the global model accounts for 92% of the variance. Space and climate contributed independently less than 6%, whereas the independent contribution of phylogeny was 10.9%. The most important contribution was found to be the interaction between the three sets (41.7%) and, to a lesser extent, the interaction between space and phylogeny (37.7%). For shell shape, the global model accounted only for 62.5% of the variance. The main independent effect was found for the phylogeny (30.5%), whereas space explained 5.7% and climate had a null independent contribution. However, the interaction between climate, space,

Table 3. Results of the model selection applied between each shell variable separately with climatic, spatial, and phylogeny predictors

	Predictors	Variables selected	wAICc	d.f.	*F*	Adjusted R^2	*P*
SH1	Climate	CC1, LGM_C2	0.362	2,16	6.714	0.388	0.007
	Space (PCNM)	1, 2, 3, 7, 8	0.244	5,13	15.15	0.797	< 0.001
	Phylogeny (PVR)	1, 2, 3, 4, 11, 17	0.242	5,13	15.86	0.856	< 0.001
SH2	Climate	LGM_C3	0.419	1,17	10.79	0.352	0.004
	Space (PCNM)	1	0.276	1,17	8.835	0.303	0.008
	Phylogeny (PVR)	1, 2, 8	0.061	3,15	6.333	0.471	0.005
SH3	Climate		0.327				
	Space (PCNM)	4, 6	0.309	2,16	10.78	0.521	0.001
	Phylogeny (PVR)	4, 7, 8, 10	0.113	4,14	9.088	0.642	< 0.001

For each shell variable, the variables retained by the model selection procedure [for space, the rank of the principal coordinates of Neighbour matrix (PCNM) and, for phylogeny, the rank of the phylogenetic eigenvector regression analysis (PVR)], the Akaike's information criterion corrected for small sample size weight (wAICc) of the best model, the degrees of freedom, the *F*-ratio and its associated *P*-value, as well as the adjusted R^2 are given. Model coefficients and their associated *P*-values for each model are given in the Supporting information (Table S5). CC, contemporary climate; LGM, last glacial maximum.

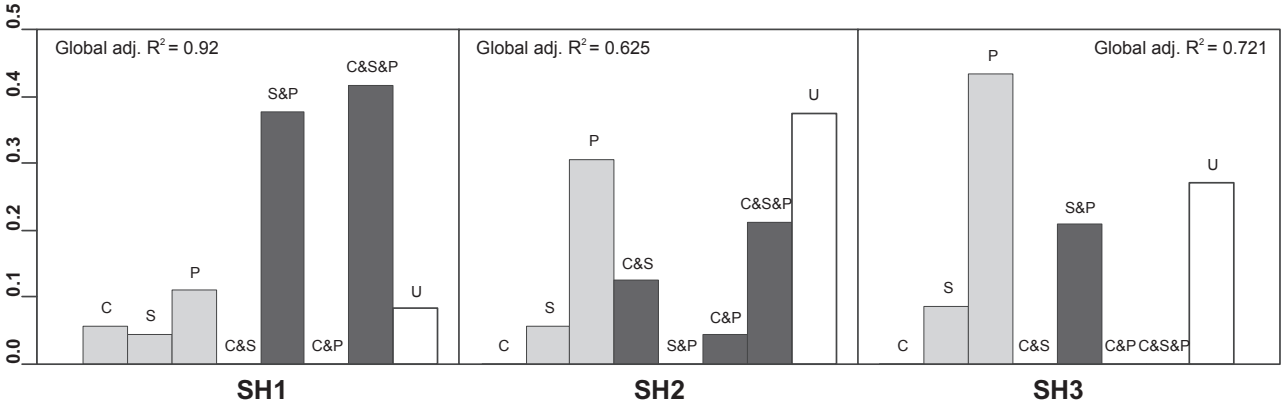

Figure 7. Fractions of adjusted percentage variation (adjusted R^2) explained for SH1, SH2, and SH3 by climate, space, and phylogeny. Horizontal bars represent the contribution of each component. Light grey represents an independent contribution and black signifies interactions. White bars correspond to the unexplained variance. C, climate; S, space; P, phylogeny; U, unexplained variance. The '&' symbol indicates the interactions. For graphical convenience, negative values of adjusted R^2 were set to 0. For details, see the Supporting information (Table S6).

and phylogeny was the most explicative one (21%), followed by the interaction between climate and space (12.4%). The others were negligible. For aperture shape, only space and phylogeny contributed to the variance (global model = 72.1%) with an independent effect of 8.6% and 43.4%, respectively, and an interaction of 20.8%.

DISCUSSION

Morphological differentiation between species

Considering the power of the specific shell variables measured in the present study to discriminate between different *Codringtonia* species, it can be seen that it is very limited. Based on the PCA results, it is evident that there are species that greatly overlap in morphological space and others that occupy the extreme ends and are clearly discriminated from each other. Both the results of the PerMANOVA based on the three axes and for each axes separately indicated that species differed significantly in their shell morphology, with differentiations being better reflected in shell size (SH1) and shell shape (SH2). The post-hoc pairwise comparisons of PerMANOVA (see Supporting information, Table S4) show significant differences being present between pairs of species. For example, along SH1, *C. codringtonii* clearly differs

from all the other species, whereas, along SH3 (aperture shape), *C. eucineta* is significantly different from the other species.

We should note that, according to Subai (2005), some *Codringtonia* species differ from others with respect to their shell colour. For example, *C. parnassia* has a pale shell with narrow brown-coloured bands whereas *C. gittenbergeri* has a shell that is brown to very dark brown, and so on. Furthermore, some species can be distinguished by other shell traits, such as the presence or not of an open umbilicus; for example, *C. intusplicata* has an open (or partly open) umbilicus, whereas the umbilicus of *C. elisabethae* and *C. gittenbergeri* is always covered. Finally, the shell sculpture (i.e. in *C. gittenbergeri*) is also used for discriminating between some *Codringtonia* species. Therefore, using a combination of shell traits as well as genitalia features, Subai (2005) reports that it is possible to delineate *Codringtonia* species (although see also Kotsakiozi *et al*., 2012). However, in the present study, we are not evaluating the taxonomic utility of the shell features. We have selected some of these features as a means to capture the shell variability of *Codringtonia* in an effort to assess the ecological and evolutionary determinants that have shaped it over the course of the genus' radiation.

Decomposition of the shell morphology along the phylogeny: the relative contribution of species and populations

Species of *Codringtonia* greatly overlap and the reason for this is the extreme shell variation exhibited within each species. The conspecific *Codringtonia* populations significantly differ from each other. This is visualized in the Supporting information (Fig. S3), where each species is presented on the PCA scatterplot separately and the morphological space and the centroid of each conspecific population is depicted. After performing a Kruskal–Wallis test between conspecific populations, it can be seen that, both in SH1 and SH2, the conspecific populations of each species are quite different from each other. Therefore, it can be claimed that each population considered in a species is significantly altering the total morphological space occupied by the species. Consequently, it is reasonable to argue that to approach the *Codringtonia*'s shell variability, both the inter- and intraspecies levels have to be considered because a single population cannot serve as a surrogate of the total shell variability exhibited by the species. This is a point that has been raised for other traits as well and, recently, (Stevens *et al*., 2010) suggested a statistical framework for considering this issue. According to their suggestion, the relative contribution of the inter- and intraspecies nodes of a phylogenetic tree to the overall shell variability can be explored. Based on Figure 4, which was generated *sensu* Stevens *et al*. (2010), it can be seen that a major burst of shell size (SH1) differentiation took place early in the radiation of the genus when the split between the species *C. intusplicata* and the ancestor species of *C. codringtonii*, *C. eucineta*, *C. gittenbergeri-elisabethae* and *C. helenae* took place. Subsequently, variation in shell size was acquired towards the tips of the phylogenetic tree, when conspecific populations diverged. The two species whose populations contribute significantly to this trend are *C. intusplicata* and *C. parnassia*. Consequently, according to this analysis, size variation in *Codringtonia* is predominantly driven by a major speciation event that occurred 3.44 Mya (Kotsakiozi *et al*., 2012). Regarding SH2 (shell shape), the relative contribution of species and populations appears somewhat more balanced compared to shell size. Shell shape variation is shown to be governed both by speciation and conspecific populations divergence events. A major shape change is recorded to have taken place when *C. codringtonii* diverged from its sister clade that comprises *C. gittenbergeri-elisabethae* and *C. helenae*, an event that occurred 2.85 Mya. However, the next shape variation burst incident was related to the divergence of *C. intusplicata* populations (1.8 Mya). Lastly, for aperture shape (SH3), all variability has occurred relatively recent and is related only to intraspecies variability. Focusing on the cladogenetic events that are recorded to have substantially contributed to the shell variability of the genus, it can be seen that they have occurred within the last 1.8–3.44 Mya. As noted in Kotsakiozi *et al*. (2012), this time interval appears to be critical for that part of mainland Greece. Around that time, Peloponnese was disconnected from Central Greece and started expanding in area towards the size it presently occupies. Similarly, this time frame coincides with the establishment of the Mediterranean climate in the region that occurred 3.2 Mya (Blondel & Aronson, 1999). Most likely, the historical process occurring in these areas of mainland Greece during that time provided the setting for the ancestor lineages of *Codringtonia* to disperse, differentiate, adapt, and speciate.

Phylogenetic signal and patterns of traits diversification

Considering only the populations of each species for which phylogenetic information (see Supporting information, Fig. S1) is available (six species, 19 populations in total), and based on the output of the PVR analysis, it can be seen that shell size (SH1) strongly

conforms to the Brownian model of trait evolution (Fig. 5). This means that variability in size increases proportionally to the phylogenetic distance (Freckleton, 2009); thus, shell size variation was mainly driven by speciation events that are by definition separated by larger phylogenetic distances than conspecific populations divergence events. Therefore, this analysis corroborates the findings reported above and highlights the fact that size variation is species related and has taken place during the early stages of the radiation of *Codringtonia*. By contrast, shell shape (SH2) appears to be diverging towards the tips of the phylogeny (Fig. 5; PSR below the linear expectation). This pattern is even more pronounced for SH3 (aperture shape). The divergence of traits towards the tips of the phylogeny, indicates absence of phylogenetic effect and this is supported by the value of K estimated for aperture shape (see results). Summarizing, this analysis is in favour of the argument that the variation in shell size is mostly species related, whereas variation in shell shape, and especially in aperture shape, is governed by conspecific populations divergence events. This result was supported by the analyses based on the framework of Stevens *et al*. (2010) as well. Viewing these results through a different perspective, it is evident that shell size is phylogenetically constrained, whereas shell shape and aperture shape are not. Therefore, these two shell traits may be the ones that populations can finely adjust to cope with the local microscale environmental conditions (i.e. microclimate of rock crevices, rock inclination, etc.) that they are faced with.

Modeling shell morphological variability: the relative contribution of climate, space, and phylogeny

In an effort to disentangle the effect of climate, phylogeny and space on the shell variability of *Codringtonia*, it was revealed that shell size (SH1) is a function of the interaction of all these three components. In the output of the model selection for space, the most important contributors are PCNM2 and PCNM3 (see Supporting information, Table S4), which both reflect the broad spatial scale that translates into great differences in latitude and longitude. Shell size was found to be negatively and significantly explained by latitude (PGLS: $R^2 = 0.39$, $F_{2,17} = 11.18$, $P < 0.001$) with larger individuals found in the south of the distributional area and smaller ones located in the north (Fig. 6). At the same time, in the phylogeny, the most important contributors are PVR1 and PVR3 (see Supporting information, Table S4), two phylogenetic filters relating to deep cladogenetic events. It has already been shown that, during the radiation of *Codringtonia*, the ancestor species dispersed southwards (Kotsakiozi *et al*., 2012) and now it is indicated that, when the species diverged towards the south, they also increased in size. *Codringtonia* species have an almost mosaic distribution and, according to the biogeographical scenario proposed for the genus by Kotsakiozi *et al*. (2012), its initial distributional area was Central Greece, and then a duplication event allowed the expansion of the genus into the adjacent area of the Peloponnese peninsula. Subsequently, a north to south colonization of the Peloponnese took place (Kotsakiozi *et al*., 2012). The southward progression of *Codringtonia* is reflected in the phylogenetic tree of the genus (see Supporting information, Fig. S1) because the distantly-related species are also distributed distantly apart on the north–south axis of the Peloponnese peninsula (Greece). Based on these findings, we argue that the strong overlap recorded between phylogeny and space in interpreting the shell size trait is fully justified. Regarding the effect of climate, it is impressive that both the contemporary and the LGM climate explain a substantial amount (38%) of the shell size variation. However, the variance partitioning analysis indicates that climate was not distinguishable from phylogeny and space in terms of variance explained for shell size, meaning that shell size and the climatic and phylogeny factors selected in the present study were all spatially structured, mainly along the latitudinal gradient (Fig. 6; see also Supporting information, Fig. S2, Table S5). At this point, we note that a small (5%; Fig. 7) but pure climatic effect on shell size is evident. For shell shape (SH2), space and phylogeny explain less variance than that which they explain for shell size. At the same time, space and climate cannot be disentangled in their contribution to shell shape. LGM climatic conditions are those that are selected as having a substantial explanatory power for shell shape, which is comparable and overlapping with the explanatory power of space. Again, the only explanation for this pattern is that both space and climate capture the same amount of variance in shell shape because climate is itself spatially structured. Regarding the aperture shape (SH3), in the output of the variance partitioning, it is mainly eigenvectors relating to middle to late cladogenetic events and small spatial variability that serve as the major contributors of its variability. The variability of aperture shape is mostly interpreted by a spatial eigenvector (PCNM4) that refers to medium spatial scale (see Supporting information, Fig. S2). Compared to shell size, which is strongly explained by deep divergence events, aperture shape is related to late diversification events. In other words, the part of the phylogeny that explains aperture shape is mainly related to recent cladogenetic events. Therefore, in the variance

partitioning analysis, the increased effect of phylogeny found for aperture shape has to be perceived as the effect of intraspecific diversification and not of deep cladogenetic events.

Regarding the effect of climate on shell and aperture shape, we should note that the climatic variables used in the present study reflect past and present climatic variations on a large scale. Therefore, the absence of climatic contribution in shell and aperture shape does not necessarily mean that climate does not have an affect on the shell and aperture shape but rather that large-scale climatic variation has no clear impact on these shell features. However, it is highly probable that small-scale climatic variations may explain substantially shell and aperture shape, although such information is currently not available.

There are several cases of land snails where climatic conditions have been found to play a major role in shaping the shell's variability (Goodfriend, 1986; Pfenninger, Eppenstein & Magnin, 2003; Parent & Crespi, 2009; Buckley *et al*., 2011). Moreover, in other globular-like rock-dwelling land snail species, it has been argued that the presence or absence of a specific feature (keel) of the shell can be an adaptation to limestone or rocky substrates (Alonso *et al*., 1985; Stankowski, 2011) or to movement through rock crevices on hard substrates (Teshima *et al*., 2003). Other studies (Cain & Cowie, 1978; Cook & Jaffar, 1984; Cameron & Cook, 1989) have shown that the shell shape (as expressed by SI or SH2 in the present study) plays a functional role leading to microhabitat preferences, with high-spired species tending to be active on steep or vertical surfaces, and low-spired species preferring low-angle or horizontal substrates. In addition, as Chiba & Kaustuv (2011) note, a theoretical model (Okajima & Chiba, 2011) of shell shape has suggested that low-spired species are optimized for locomotion on horizontal surfaces, whereas both low- and high-spired species can be well balanced on vertical surfaces. Therefore, besides climatic conditions, it is possible that the overall variation in the *Codringtonia* shell reflects adaptations dictated by the availability of limestone substrates that could be vertical or horizontal, and, accordingly, the shell adapts either to provide proper traction on the available surface or allow the snails to seek refuge within the rock fissures (Moreno-Rueda, 2006). It is reasonable to assume that the microclimatic gradient that the *Codringtonia* populations are experiencing is not captured by the bioclimatic records used in our analyses. Moreover, the spatial variables that we have used do not account for the small-scale topographical complexity of the study area. Therefore, there are additional spatial and climatic features that are not incorporated into our analyses that could theoretically be affecting the overall shell variability, especially in the level of populations. Consequently, to fully disentangle the effect of climate and space on the variability of the composite shell traits SH1 (shell size), SH2 (shell shape), and SH3 (aperture shape) of *Codringtonia*, a more spatially fine-scaled study assessing the local microclimate and the topographical complexity of the area where *Codringtonia* populations are distributed should be performed. As recently shown, scale is of major importance for revealing the evolutionary patterns of shell shapes of land snails (Fiorentino *et al*., 2013). However, even in a fine-scale study, the effect of past climatic and topographical conditions might still remain elusive if palaeoclimatic and palaeogeographic data are not available for the study region.

Conclusions

Based on the measured shell variables, there are *Codringtonia* species that greatly overlap in the morphological space, as well as others that occupy the extreme ends and are clearly discriminated from each other. A latitudinal gradient in the overall shell size of *Codringtonia* species is evident. Species of smaller size are found north, whereas larger are found south. A single population per species cannot serve as the surrogate of the total shell variability exhibited by the species. Therefore, intraspecies divergence of shell traits should be considered in land snail studies investigating trait evolution in space and time. The overall shell size of *Codringtonia* clades, is phylogenetically constrained, related to early speciation events, and strongly affected by large-scale spatial variability. The effect of climate on this trait cannot be disentangled from phylogeny and space. Shell shape and aperture shape are not phylogenetically constrained; they appear to have diversified mostly towards the middle and the late part of genus radiation, thus relating mostly to population divergence. Late divergence is especially true for aperture shape. Shell shape is substantially explained by both climate and space that greatly overlap. Finally, aperture shape is mainly interpreted by medium- to small-scale spatial variables. Fully disentangling the effect of climate and space on shell variability probably requires the incorporation of spatial and climate small-scale local conditions.

ACKNOWLEDGEMENTS

We would like to thank Sinos Giokas and Eike Neubert for providing *Codringtonia* specimens from their personal collections. We also wish to express our gratitude to Katerina Vardinoyannis (Natural History Museum of Crete, NHMC), Edmund Gittenberger (Naturalis Biodiversity Center, NBC), Jeroen Goud

(NBC), A. N. van der Bijl (NBC), Ronald Janssen (Senckenberg), Jonathan Ablett (Natural History Museum London, NHM), and Christine Zorn (Zoologisches Museum Berlin, ZMB) for providing or mediating to gain access to valuable *Codringtonia* specimens (or shell photos) maintained in the respective institutes. Our most sincere thanks are extended to Robert Cameron, Gregorio Moreno-Rueda, and an anonymous reviewer who provided comments that greatly improved our manuscript.

REFERENCES

Alonso MR, Alcantara L, Rivas P, Ibanez M. 1985. A biogeographic study of *Iberus gualterianus* (L.) (Pulmonata: Helicidae). *Soosiana* **13:** 1–10.

Anderson MJ. 2006. Distance-based tests for homogeneity of multivariate dispersions. *Biometrics* **62:** 245–253.

Bardají T, Goy JL, Zazo C, Hillaire-Marcel C, Dabrio CJ, Cabero A, Ghaleb B, Silva PG, Lario J. 2009. Sea level and climate changes during OIS 5e in the Western Mediterranean. *Geomorphology* **104:** 22–37.

Barton K. 2013. *Package 'MuMIn'*. Available at: http://r-forge.r-project.org/projects/mumin/

Blomberg SP, Garland T, Ives AR. 2003. Testing for phylogenetic signal in comparative data: behavioral traits are more labile. *Evolution* **57:** 717–745.

Blondel J, Aronson J. 1999. *Biology and wildlife of the Mediterranean region*. Oxford: Oxford University Press.

Borcard D, Legendre P. 2002. All-scale spatial analysis of ecological data by means of principal coordinates of neighbour matrices. *Ecological Modelling* **153:** 51–68.

Borcard D, Legendre P, Avois-Jacquet C, Tuomisto H. 2004. Dissecting the spatial structure of ecological data at multiple scales. *Ecology* **85:** 1826–1832.

Buckley TR, Stringer I, Gleeson D, Howitt R, Attanayake D, Parrish R, Sherley G, Rohan M. 2011. A revision of the New Zealand *Placostylus* land snails using mitochondrial DNA and shell morphometric analyses, with implications for conservation. *New Zealand Journal of Zoology* **38:** 55–81.

Burla H. 1984. Induced environmental variation in *Arianta arbustorum* (L.). *Genetica* **64:** 65–67.

Cain AJ, Cowie RH. 1978. Activity of different species of land-snail on surfaces of different inclinations. *Journal of Conchology* **29:** 267–272.

Cameron RAD. 2013. The diversity of land molluscs-questions unanswered and questions unasked. *American Malacological Bulletin* **31:** 169–180.

Cameron RAD, Cook LM. 1989. Shell size and shape in Madeiran land snails: do niches remain unfilled? *Biological Journal of the Linnean Society* **36:** 79–96.

Cameron RAD, Cook LM, Gao G. 1996. Variation in snail species widespread on Porto Santo, Madeiran archipelago. *Journal of Molluscan Studies* **62:** 143–150.

Cameron RAD, Pokryszko BM, Horsák M, Sirbu I, Gheoca V. 2011. Forest snail faunas from Transylvania (Romania) and their relationship to the faunas of Central and Northern Europe. *Biological Journal of the Linnean Society* **104:** 471–479.

Chiba S. 1996. Ecological and morphological diversification within single species and character displacement in *Mandarina*, endemic land snails of the Bonin Islands. *Journal of Evolutionary Biology* **9:** 277–291.

Chiba S, Kaustuv R. 2011. Selectivity of terrestrial gastropod extinctions on an oceanic archipelago and insights into the anthropogenic extinction process. *Proceedings of the National Academy of Sciences of the United States of America* **108:** 9496–9501.

Cliff AD, Ord JK. 1981. *Spatial processes: models and applications*. London: Pion Limited.

Cook LM, Jaffar WN. 1984. Spire index and preferred surface orientation in some land snails. *Biological Journal of the Linnean Society* **21:** 307–313.

Diniz Filho JAF, Rangel TF, Santos T, Bini LM. 2012. Exploring patterns of interspecific variation in quantitative traits using sequential phylogenetic eigenvector regressions. *Evolution* **66:** 1079–1090.

Diniz-Filho JAF, De Sant' Ana CER, Bini LM. 1998. An eigenvector method for estimating phylogenetic inertia. *Evolution* **52:** 1247–1262.

Fiorentino V, Manganelli G, Giusti F, Tiedemann R, Ketmaier V. 2013. A question of time: the land snail *Murella muralis* (Gastropoda: Pulmonata) reveals constraints on past ecological speciation. *Molecular Ecology* **22:** 170–186.

Freckleton RP. 2009. The seven deadly sins of comparative analysis. *Journal of Evolutionary Biology* **22:** 1367–1375.

Garamszegi LZ, Møller AP. 2010. Effects of sample size and intraspecific variation in phylogenetic comparative studies: a meta-analytic review. *Biological Reviews* **85:** 797–805.

Garland JT, Ives AR. 2000. Using the past to predict the present: confidence intervals for regression equations in phylogenetic comparative methods. *American Naturalist* **155:** 346–364.

Garland T, Bennett JAF, Rezende EL. 2005. Phylogenetic approaches in comparative physiology. *Journal of Experimental Biology* **208:** 3015–3035.

Goodfriend GA. 1986. Variation in land-snail shell form and size and its causes – a review. *Systematic Zoology* **35:** 204–223.

Hardy OJ, Pavoine S. 2012. Assessing phylogenetic signal with measurement error: a comparison of Mantel tests, Blomberg *et al.*'s *K*, and phylogenetic distograms. *Evolution* **66:** 2614–2621.

Hausdorf B. 2003. Latitudinal and altitudinal body size variation among north-west European land snail species. *Global Ecology & Biogeography* **12:** 389–394.

Hijmans RJ, Cameron SE, Parra JL, Jones PG, Jarvis A. 2005. WORLDCLIM – a set of global climate layers (climate grids). *International Journal of Climatology* **25:** 1965–1978.

Holm S. 1979. A simple sequentially rejective multiple test procedure. *Scandinavian Journal of Statistics* **6:** 65–70.

Ives AR, Midford PE, Garland T. 2007. Within-species variation and measurement error in phylogenetic comparative methods. *Systematic Biology* **56:** 252–270.

Johnson MS. 2011. Thirty-four years of climatic selection in the land snail *Theba pisana*. *Heredity* **106:** 741–748.

Jordaens K, Van Riel P, Frias AM, Backeljau T. 2009. Speciation on the Azores islands: congruent patterns in shell morphology, genital anatomy, and molecular markers in endemic land snails (Gastropoda, Leptaxinae). *Biological Journal of the Linnean Society* **97:** 166–176.

Kappes H, Jordaens K, Van Houtte N, Hendrickx F, Maelfait J-P, Lens L, Backeljau T. 2009. A land snail's view of a fragmented landscape. *Biological Journal of the Linnean Society* **98:** 839–850.

Kotsakiozi P, Parmakelis A, Giokas S, Papanikolaou I, Valakos ED. 2012. Mitochondrial phylogeny and biogeographic history of the Greek endemic land-snail genus *Codringtonia* Kobelt 1898 (Gastropoda, Pulmonata, Helicidae). *Molecular Phylogenetics and Evolution* **62:** 681–692.

Legendre P, Legendre P. 1998. *Numerical ecology*. Amsterdam: Elsevier Science.

Moreno-Rueda G. 2006. Habitat use by the arid-dwelling land snail *Iberus g. gualtieranus*. *Journal of Arid Environments* **67:** 336–342.

Neter J, Wasserman W, Kutner MH. 1990. *Applied linear statistical models: regression, analysis of variance, and experimental designs*. Homewood, IL: Irwin.

Okajima R, Chiba S. 2011. How does life adapt to a gravitational environment? The outline of the terrestrial gastropod shell. *American Naturalist* **178:** 801–809.

Oksanen J, Kindt R, Legendre P, O'Hara B, Stevens MHH, Oksanen MJ, Suggests MASS. 2007. *The vegan package. Community ecology package*. Available at: http://r-forge.r-project.org/projects/vegan/

Paradis E, Claude J, Strimmer K. 2004. APE: analyses of phylogenetics and evolution in R language. *Bioinformatics* **20:** 289–290.

Parent CE, Crespi BJ. 2009. Ecological opportunity in adaptive radiation of Galapagos endemic land snails. *American Naturalist* **174:** 898–905.

Pavoine S, Baguette M, Bonsall MB. 2010. Decomposition of trait diversity among the nodes of a phylogenetic tree. *Ecological Monographs* **80:** 485–507.

Pfenninger M. 2004. Comparative analysis of range sizes in Helicidae s.l. (Pulmonata, Gastropoda). *Evolutionary Ecology Research* **6:** 359–376.

Pfenninger M, Eppenstein A, Magnin F. 2003. Evidence for ecological speciation in the sister species *Candidula unifasciata* (Poiret, 1801) and *C. rugosiuscula* (Michaud, 1831) (Helicellinae, Gastropoda). *Biological Journal of the Linnean Society* **79:** 611–628.

R Development Core Team. 2011. *R: A Language and Environment for Statistical Computing*. Vienna: R Foundation for Statistical Computing.

Rao CR. 1982. Diversity and dissimilarity coefficients: a unified approach. *Theoretical Population Biology* **21:** 24–43.

Revell LJ. 2012. Phytools: an R package for phylogenetic comparative biology (and other things). *Methods in Ecology and Evolution* **3:** 217–223.

Ricklefs RE. 2012. Species richness and morphological diversity of passerine birds. *Proceedings of the National Academy of Sciences of the United States of America* **109:** 14482–14487.

Santos T, Diniz-Filho JAF, Rangel T, Bini LM. 2012. *Package 'PVR'*. Available at: http://cran.r-project.org/web/packages/PVR/index.html

Schluter D, ed. 2006. *The ecology of adaptive radiation*. Oxford: Oxford University Press.

Stankowski S. 2011. Extreme, continuous variation in an island snail: local diversification and association of shell form with the current environment. *Biological Journal of the Linnean Society* **104:** 756–769.

Stevens VM, Pavoine S, Baguette M. 2010. Variation within and between closely related species uncovers high intra-specific variability in dispersal. *PLoS ONE* **5:** e11123.

Subai P. 2005. Revision of the genus *Codringtonia* Kobelt 1898 (Gastropoda: Pulmonata: Helicidae: Helicelinae). *Archiv fuer Molluskenkunde* **134:** 65–119.

Sugiura N. 1978. Further analysis of the data by Akaike's information criterion and the finite corrections. *Communications in Statistics-Theory and Methods* **7:** 13–26.

Suvorov AN. 2002. Prospects for studies of morphological variability of land pulmonates snails. *Biology Bulletin of the Russian Academy of Sciences* **29:** 455–467.

Teshima H, Davison A, Kuwahara Y, Yokoyama J, Chiba S, Fukuda T, Ogimura H, Kawata M. 2003. The evolution of extreme shell shape variation in the land snail *Ainohelix editha*: a phylogeny and hybrid zone analysis. *Molecular Ecology* **12:** 1869–1878.

SUPPORTING INFORMATION

Additional Supporting Information may be found in the online version of this article at the publisher's web-site:

Figure S1. The ultrametric tree of *Codringtonia* populations obtained after pruning the respective tree of Kotsakiozi *et al*. (2012). Branch lengths are expressed in million years. The dashed rectangles encompass each species' populations. Black and grey dots on nodes indicate inter- and intraspecies splits, respectively.

Figure S2. Plots of the 11 principal coordinates of Neighbour matrices (PCNMs) inferred for the study area. PCNMs are eigenvectors derived from a principal coordinate analysis applied on the truncated matrix of geographical distances calculated using the latitude and longitude of the studied sites. The circles represent the centered-scaled PCNM eigenvector site scores (mean = 0, SD = 1) with positive (black circles) and negative (white circles) values proportional in area to the absolute value.

Figure S3. Scatter-plot of the scores of the principal component analysis (PCA) on the first two principal components accounting for 77.8% of the total shell variation of each population of each *Codringtonia* species studied. The polygons define the morphological space occupied by each population and the red dots correspond to the centroid of each morphological space. The *p*-values of the Kruskal–Wallis tests (KW) performed between populations for each PC axis are given on the bottom right of each scatter plot.

Table S1. Species and populations included in the present study

Table S2. List of the 19 climatic variables extracted from WorldClim for contemporary climate and Last Glacial Maximum with their ranges (inferred from the sampled populations)

Table S3. The contribution (loadings) of each climatic variable on the first three principal component axes for contemporary climate (CC1, CC2, and CC3), Last Glacial Maximum (LGM) estimated by both the Community Climate System Model (LGM_C1, LGM_C2, and LGM_C3) and the Model for Interdisciplinary Research on Climate (LGM_M1, LGM_M2, and LGM_M3)

Table S4. *P*-values of the post-hoc pairwise permutational multivariate analysis of variance tests corrected for multiple tests.

Table S5. Model coefficients for the best model according to the model selection procedure for each shell variable and for each set of predictors.

Table S6. Results of the variance partitioning (i.e. expressed as adjusted R^2 between climate, space, and phylogenetic effect for each shell variables)